Rayleigh's Classical Damping Revisited

Sondipon Adhikari[1]
University of Bristol, Bristol, United Kingdom

A. Srikantha Phani[2]
University of Cambridge, Cambridge, United Kingdom

ABSTRACT

Proportional damping is a widely used approach to model dissipative forces in complex engineering structures and it has been used in various dynamic problems for more than ten decades. A major limitation of the mass and stiffness proportional damping approximation is the lack of generality of the model to allow for experimentally observed variation of damping factors with respect to vibration frequency in complex structures. To remedy this, a new generalized proportional damping model is proposed. The proposed method requires only the measurements of natural frequencies and modal damping factors which can be obtained using a point measurement of the frequency response function (FRF). Simulation examples are provided to illustrate the proposed method. Verification of the proposed technique in lab scale experiments is presented. It is concluded that the present method has significant potential in modelling damping in industrial scale structures.

INTRODUCTION

Modal analysis is the most popular and efficient method for solving engineering dynamic problems. The concept of modal analysis, as introduced by Lord Rayleigh (1877), was originated from the linear dynamics of undamped systems. The undamped modes or classical normal modes satisfy an orthogonality relationship over the mass and stiffness matrices and uncouple the equations of motion, *i.e.*, if $\mathbf{\Phi}$ is the modal matrix then $\mathbf{\Phi}^T\mathbf{M}\mathbf{\Phi}$ and $\mathbf{\Phi}^T\mathbf{K}\mathbf{\Phi}$ are both diagonal matrices. This significantly simplifies the dynamic analysis because complex multiple degree-of-freedom (MDOF) systems can be effectively treated as a collection of single degree-of-freedom oscillators.

Real-life systems are not undamped but possess some kind of energy dissipation mechanism or damping. In order to apply modal analysis of undamped systems to damped systems, it is common to assume the proportional damping, a special type of viscous damping. The proportional damping model expresses the damping matrix as a linear combination of the mass and stiffness matrices, that is

$$\mathbf{C} = \alpha_1\mathbf{M} + \alpha_2\mathbf{K} \tag{1}$$

where α_1, α_2 are real scalars. This damping model is also known as 'Rayleigh damping' or 'classical damping'. Modes of classically damped systems preserve the simplicity of the real normal modes as in the undamped case. Caughey and O'Kelly (1965) have derived the condition which the system matrices must satisfy so that viscously damped linear systems possess classical normal modes. They have also proposed a series expression for the damping matrix in terms of the mass and stiffness matrices so that the system can be decoupled by the undamped modal matrix and have shown that the Rayleigh damping is a special case of this general expression. In this paper a more general expression of the damping matrix is proposed while retaining the advantage of classical normal modes.

Complex engineering structures in general have non-proportional damping. For a non-proportionally damped system, the equations of motion in the modal coordinates are coupled through the off-diagonal terms of the modal damping matrix and consequently the system possesses complex modes instead of real normal modes. Practical experience in modal testing also shows that most real-life structures possess complex modes. Complex modes can arise for various other reasons also (Phani, 2004), for example, due to the gyroscopic effects, aerodynamic effects, nonlinearity and experimental noise. Adhikari and Woodhouse (2001a,b) have proposed few methods to identify damping from experimentally identified complex modes. In spite of a large amount of research, understanding and identification of complex modes is not well developed as real normal modes. The main reasons are:

[1]Lecturer, Department of Aerospace Engineering, University of Bristol, Queens Building, University Walk, Bristol BS8 1TR, UK, AIAA Member.

[2]Research Associate, Department of Engineering, University of Cambridge, Trumpington Street, Cambridge CB2 1PZ, UK.

- In contrast with real normal modes, the 'shapes' of complex modes are not in general clear. It appears that unlike the (real) scaling of real normal modes, the (complex) scaling or normalization of complex modes has a significant effect on their geometric appearance. This makes it particularly difficult to experimentally identify complex modes in a consistent manner (Adhikari, 2004).
- The imaginary parts of the complex modes are usually very small compared to the real parts, especially when the damping is small. This makes it difficult to reliably extract complex modes using numerical optimization methods in conjunction with experimentally obtained transfer function residues. A minimum phase scaling has be suggested by Phani (2004) which has the distinct advantage that the real part of the damped complex mode is closest to the undamped real mode.
- The phase of complex modes are highly sensitive to experimental errors and hence not reliable.

In order to bypass these difficulties, often real normal modes are used in experimental modal analysis. Chen et al. (1996), Ibrahim (1983), and Balmès (1997) have proposed methods to obtain the best real normal modes from identified complex modes. The damping identification method proposed in this paper assumes that the system is effectively proportionally damped so that the complex modes can be neglected. The outline of the paper is as follows. In section 3, a background of proportionally damped systems is provided. The concept of generalized proportional damping is introduced in section 4. The damping identification method using the generalized proportional damping is discussed in section 5. Based on the proposed damping identification technique, a general method of modelling of damping for complex systems has been outlined in section 6. Numerical examples are provided to illustrate the proposed approach.

BACKGROUND OF PROPORTIONALLY DAMPED SYSTEMS

The equations of motion of free vibration of a viscously damped system can be expressed by

$$\mathbf{M}\ddot{\mathbf{q}}(t) + \mathbf{C}\dot{\mathbf{q}}(t) + \mathbf{K}\mathbf{q}(t) = \mathbf{0}. \tag{2}$$

Caughey and O'Kelly (1965) have proved that a damped linear system of the form (2) can possess classical normal modes if and only if the system matrices satisfy the relationship $\mathbf{K}\mathbf{M}^{-1}\mathbf{C} = \mathbf{C}\mathbf{M}^{-1}\mathbf{K}$. This is an important result on modal analysis of viscously damped systems and is now well known. However, this result does not immediately generalize to systems with singular mass matrices (Newland, 1989). This apparent restriction in Caughey and O'Kelly's result may be removed by considering the fact that all the three system matrices can be treated on equal basis and therefore can be interchanged. In view of this, when the system matrices are non-negative definite we have the following theorem:

Theorem 1. *A viscously damped linear system can possess classical normal modes if and only if at least one of the following conditions is satisfied:*
(a) $\mathbf{K}\mathbf{M}^{-1}\mathbf{C} = \mathbf{C}\mathbf{M}^{-1}\mathbf{K}$, *(b)* $\mathbf{M}\mathbf{K}^{-1}\mathbf{C} = \mathbf{C}\mathbf{K}^{-1}\mathbf{M}$, *(c)* $\mathbf{M}\mathbf{C}^{-1}\mathbf{K} = \mathbf{K}\mathbf{C}^{-1}\mathbf{M}$.

This can be easily proved by following Caughey and O'Kelly's approach and interchanging $\mathbf{M}$, $\mathbf{K}$ and $\mathbf{C}$ successively. If a system is $(\bullet)$-singular then the condition(s) involving $(\bullet)^{-1}$ have to be disregarded and remaining condition(s) have to be used. Thus, for a positive definite system, along with Caughey and O'Kelly's result (condition (a) of the theorem), there exist two other equivalent criterion to judge whether a damped system can possess classical normal modes. It is important to note that these three conditions are equivalent and simultaneously valid but in general *not* the same.

Example 1.

Assume that a system's mass, stiffness and damping matrices are given by

$$\mathbf{M} = \begin{bmatrix} 1.0 & 1.0 & 1.0 \\ 1.0 & 2.0 & 2.0 \\ 1.0 & 2.0 & 3.0 \end{bmatrix}, \quad \mathbf{K} = \begin{bmatrix} 2 & -1 & 0.5 \\ -1 & 1.2 & 0.4 \\ 0.5 & 0.4 & 1.8 \end{bmatrix} \quad \text{and} \quad \mathbf{C} = \begin{bmatrix} 15.25 & -9.8 & 3.4 \\ -9.8 & 6.48 & -1.84 \\ 3.4 & -1.84 & 2.22 \end{bmatrix}. \tag{3}$$

It may be verified that all the system matrices are positive definite. The mass-normalized undamped modal matrix is obtained as

$$\mathbf{\Phi} = \begin{bmatrix} 0.4027 & -0.5221 & -1.2511 \\ 0.5845 & -0.4888 & 1.1914 \\ -0.1127 & 0.9036 & -0.4134 \end{bmatrix}. \tag{4}$$

Since Caughey and O'Kelly's condition

$$\mathbf{K}\mathbf{M}^{-1}\mathbf{C} = \mathbf{C}\mathbf{M}^{-1}\mathbf{K} = \begin{bmatrix} 125.45 & -80.92 & 28.61 \\ -80.92 & 52.272 & -18.176 \\ 28.61 & -18.176 & 7.908 \end{bmatrix}$$

is satisfied, the system possess classical normal modes and that $\mathbf{\Phi}$ given in equation (4) is the modal matrix. Because the system is positive definite the other two conditions,

$$\mathbf{M}\mathbf{K}^{-1}\mathbf{C} = \mathbf{C}\mathbf{K}^{-1}\mathbf{M} = \begin{bmatrix} 2.0 & -1.0 & 0.5 \\ -1.0 & 1.2 & 0.4 \\ 0.5 & 0.4 & 1.8 \end{bmatrix}$$

and

$$\mathbf{M}\mathbf{C}^{-1}\mathbf{K} = \mathbf{K}\mathbf{C}^{-1}\mathbf{M} = \begin{bmatrix} 4.1 & 6.2 & 5.6 \\ 6.2 & 9.73 & 9.2 \\ 5.6 & 9.2 & 9.6 \end{bmatrix}$$

are also satisfied. Thus all three conditions described in Theorem 1 are simultaneously valid although none of them are the same. So, if any one of the three conditions proposed in Theorem 1 is satisfied, a viscously damped positive definite system possesses classical normal modes.

Example 2.

Suppose for a system

$$\mathbf{M} = \begin{bmatrix} 7.0584 & 1.3139 \\ 1.3139 & 0.2446 \end{bmatrix}, \quad \mathbf{K} = \begin{bmatrix} 3.0 & -1.0 \\ -1.0 & 4.0 \end{bmatrix} \quad \text{and} \quad \mathbf{C} = \begin{bmatrix} 1.0 & -1.0 \\ -1.0 & 3.0 \end{bmatrix}. \tag{5}$$

It may be verified that the mass matrix is singular for this system. For this reason, Caughey and O'Kelly's criteria is not applicable. But, as the other two conditions in Theorem 1,

$$\mathbf{M}\mathbf{K}^{-1}\mathbf{C} = \mathbf{C}\mathbf{K}^{-1}\mathbf{M} = \begin{bmatrix} 1.6861 & 0.3139 \\ 0.3139 & 0.0584 \end{bmatrix}$$

and

$$\mathbf{M}\mathbf{C}^{-1}\mathbf{K} = \mathbf{K}\mathbf{C}^{-1}\mathbf{M} = \begin{bmatrix} 29.5475 & 5.5 \\ 5.5 & 1.0238 \end{bmatrix}$$

are satisfied, all three matrices can be diagonalized by a congruence transformation using the undamped modal matrix

$$\mathbf{\Phi} = \begin{bmatrix} 0.9372 & -0.1830 \\ 0.3489 & 0.9831 \end{bmatrix}.$$

GENERALIZED PROPORTIONAL DAMPING

In spite of a large amount of research, the understanding of damping forces in vibrating structures is not well developed. A major reason for this is that, by contrast with inertia and stiffness forces, the physics behind the damping forces is in general not clear. As a consequence, obtaining a damping matrix from the first principles is difficult, if not impossible, for real-life engineering structures. For this reason, assuming $\mathbf{M}$ and $\mathbf{K}$ are known, we often want to express $\mathbf{C}$ in terms of $\mathbf{M}$ and $\mathbf{K}$ such that the system still possesses classical normal modes. Of course, the earliest work along this line is the proportional damping shown in equation (1) by Rayleigh (1877). It may be verified that expressing $\mathbf{C}$ in such a way will always satisfy the conditions given by Theorem 1. Caughey (1960) proposed that a *sufficient* condition for the existence of classical normal modes is: if $\mathbf{M}^{-1}\mathbf{C}$ can be expressed in a series involving powers of $\mathbf{M}^{-1}\mathbf{K}$. His result

generalized Rayleigh's result, which turns out to be the first two terms of the series. Later, Caughey and O'Kelly (1965) proved that the series representation of damping

$$\mathbf{C} = \mathbf{M} \sum_{j=0}^{N-1} \alpha_j \left(\mathbf{M}^{-1}\mathbf{K}\right)^j \tag{6}$$

is the *necessary and sufficient* condition for existence of classical normal modes for systems without any repeated roots. This series is now known as the 'Caughey series' and is possibly the most general form of damping matrix under which the system will still possess classical normal modes.

Assuming that the system is positive definite, a further generalized and useful form of proportional damping will be proposed in this paper. Consider the conditions (a) and (b) of Theorem 1; premultiplying (a) by $\mathbf{M}^{-1}$ and (b) by $\mathbf{K}^{-1}$ one has

$$\begin{aligned} \left(\mathbf{M}^{-1}\mathbf{K}\right)\left(\mathbf{M}^{-1}\mathbf{C}\right) &= \left(\mathbf{M}^{-1}\mathbf{C}\right)\left(\mathbf{M}^{-1}\mathbf{K}\right) \quad \text{or} \quad \mathbf{AB} = \mathbf{BA} \\ \left(\mathbf{K}^{-1}\mathbf{M}\right)\left(\mathbf{K}^{-1}\mathbf{C}\right) &= \left(\mathbf{K}^{-1}\mathbf{C}\right)\left(\mathbf{K}^{-1}\mathbf{M}\right) \quad \text{or} \quad \mathbf{AD} = \mathbf{DA}, \end{aligned} \tag{7}$$

where $\mathbf{A} = \mathbf{M}^{-1}\mathbf{K}$, $\mathbf{B} = \mathbf{M}^{-1}\mathbf{C}$ and $\mathbf{D} = \mathbf{K}^{-1}\mathbf{C}$. Notice that condition (c) of Theorem 1 has not been considered. Premultiplying (c) by $\mathbf{C}^{-1}$, one would obtain a similar commutative condition. Because it would involve $\mathbf{C}$ terms in both the matrices, any meaningful expression of $\mathbf{C}$ in terms of $\mathbf{M}$ and $\mathbf{K}$ will be difficult to deduce. For this reason only the two commutative relationships in equation (7) will be considered. The eigenvalues of $\mathbf{A}$, $\mathbf{B}$ and $\mathbf{D}$ are positive due to the positive-definitiveness assumption of the system matrices. For any two matrices $\mathbf{A}$ and $\mathbf{B}$, if $\mathbf{A}$ commutes with $\mathbf{B}$, $\beta(\mathbf{A})$ also commutes with $\mathbf{B}$ where the real function $\beta(x)$ is smooth and analytic in the neighborhood of all the eigenvalues of $\mathbf{A}$. Thus, in view of the commutative relationships in equation (7), one can use several well known functions to represent $\mathbf{M}^{-1}\mathbf{C}$ in terms of $\mathbf{M}^{-1}\mathbf{K}$ and also $\mathbf{K}^{-1}\mathbf{C}$ in terms of $\mathbf{K}^{-1}\mathbf{M}$. This implies that representations like $\mathbf{C} = \mathbf{M}\,\beta(\mathbf{M}^{-1}\mathbf{K})$ and $\mathbf{C} = \mathbf{K}\,\beta(\mathbf{K}^{-1}\mathbf{M})$ are valid expressions. The damping matrix can be expressed by adding these two quantities as

$$\mathbf{C} = \mathbf{M}\,\beta_1\left(\mathbf{M}^{-1}\mathbf{K}\right) + \mathbf{K}\,\beta_2\left(\mathbf{K}^{-1}\mathbf{M}\right) \tag{8}$$

such that the system possesses classical normal modes. Postmultiplying condition (a) of Theorem 1 by $\mathbf{M}^{-1}$ and (b) by $\mathbf{K}^{-1}$ one has

$$\begin{aligned} \left(\mathbf{K}\mathbf{M}^{-1}\right)\left(\mathbf{C}\mathbf{M}^{-1}\right) &= \left(\mathbf{C}\mathbf{M}^{-1}\right)\left(\mathbf{K}\mathbf{M}^{-1}\right) \\ \left(\mathbf{M}\mathbf{K}^{-1}\right)\left(\mathbf{C}\mathbf{K}^{-1}\right) &= \left(\mathbf{C}\mathbf{K}^{-1}\right)\left(\mathbf{M}\mathbf{K}^{-1}\right). \end{aligned} \tag{9}$$

Following a similar procedure we can express the damping matrix in the form

$$\mathbf{C} = \beta_3\left(\mathbf{K}\mathbf{M}^{-1}\right)\mathbf{M} + \beta_4\left(\mathbf{M}\mathbf{K}^{-1}\right)\mathbf{K} \tag{10}$$

such that system (2) possesses classical normal modes. The functions $\beta_i(\bullet)$ should be analytic in the neighborhood of all the eigenvalues of their argument matrices. This implies that $\beta_1(\bullet)$ and $\beta_3(\bullet)$ should be analytic around ω_j^2, $\forall\, j$ and $\beta_1(\bullet)$ and $\beta_3(\bullet)$ should be analytic around $1/\omega_j^2$, $\forall\, j$. Clearly these functions can have very general forms. However, the expressions of $\mathbf{C}$ in equations (8) and (10) get restricted because of the special nature of the *arguments* in the functions. As a consequence, $\mathbf{C}$ represented in (8) or (10) does not cover the whole $\mathbb{R}^{N\times N}$, which is well known that many damped systems do not possess classical normal modes.

Rayleigh's result (1) can be obtained directly from equation (8) or (10) as a special case by choosing each matrix function $\beta_i(\bullet)$ as a real scalar times an identity matrix, that is

$$\beta_i(\bullet) = \alpha_i \mathbf{I}. \tag{11}$$

The damping matrix expressed in equation (8) or (10) provides a new way of interpreting the 'Rayleigh damping' or 'proportional damping' where the scalar constants α_i associated with $\mathbf{M}$ and $\mathbf{K}$ are replaced by arbitrary matrix functions $\beta_i(\bullet)$ with proper arguments. This kind of damping model will be called *generalized proportional damping*. We call the representation in equation (8) *right-functional form* and that

in equation (10) *left-functional form*. The functions $\beta_i(\bullet)$ will be called as *proportional damping functions* which are consistent with the definition of proportional damping constants (α_i) in Rayleighs model.

It is well known that for any matrix $\mathbf{A} \in \mathbb{R}^{N\times N}$, all $\mathbf{A}^k$, for integer $k > N$, can be expressed as a linear combination of $\mathbf{A}^j, j \leq (N-1)$ by a recursive relationship using the Cayley-Hamilton theorem (Kreyszig, 1999). Because all analytic functions have a power series form via Taylor series expansion, the expression of $\mathbf{C}$ in (8) or (10) can in turn be represented in the form of Caughey series (6). However, since all $\beta_i(\bullet)$ can have very general forms, such a representation may not be always straightforward. For example, if $\mathbf{C} = \mathbf{M}(\mathbf{M}^{-1}\mathbf{K})^{-e}$ the system possesses normal modes, but it is neither a direct member of Caughey series (6) nor is it a member of the series involving rational fractional powers given by Caughey (1960) as e is an irrational number. However, we know that $e = 1 + \frac{1}{1!} + \cdots + \frac{1}{r!} + \cdots \infty$, from which we can write $\mathbf{C} = \mathbf{M}(\mathbf{M}^{-1}\mathbf{K})^{-1}(\mathbf{M}^{-1}\mathbf{K})^{-\frac{1}{1!}} \cdots (\mathbf{M}^{-1}\mathbf{K})^{-\frac{1}{r!}} \cdots \infty$, which can in principle be represented by Caughey series. From a practical point of view it is easy to verify that, this representation is not simple and requires truncation of the series up to some finite number of terms. Therefore, the damping matrix expressed in the form of equation (8) or (10) is a more convenient representation of Caughey series. From this discussion we have the following general result for damped linear systems:

Theorem 2. *Viscously damped positive definite linear systems will have classical normal modes if and only if the damping matrix can be represented by*
(a) $\mathbf{C} = \mathbf{M}\,\beta_1\left(\mathbf{M}^{-1}\mathbf{K}\right) + \mathbf{K}\,\beta_2\left(\mathbf{K}^{-1}\mathbf{M}\right)$, *or*
(b) $\mathbf{C} = \beta_3\left(\mathbf{K}\mathbf{M}^{-1}\right)\mathbf{M} + \beta_4\left(\mathbf{M}\mathbf{K}^{-1}\right)\mathbf{K}$
where $\beta_i(\bullet)$ *are smooth analytic functions in the neighborhood of all the eigenvalues of their argument matrices.*

A proof of the theorem is given in the appendix. For symmetric positive-definite systems both expressions are equivalent and in the rest of the paper only the right functional form (a) will be considered.

Example 3.

This example is chosen to show the general nature of the proportional damping functions which can be used within the scope of conventional modal analysis. It will be shown that the linear dynamic system satisfying the following equation of free vibration

$$\begin{aligned}\mathbf{M}\ddot{\mathbf{q}} + \Big[&\mathbf{M}e^{-\left(\mathbf{M}^{-1}\mathbf{K}\right)^2/2}\sinh(\mathbf{K}^{-1}\mathbf{M}\ln(\mathbf{M}^{-1}\mathbf{K})^{2/3}) \\ &+ \mathbf{K}\cos^2(\mathbf{K}^{-1}\mathbf{M})\sqrt[4]{\mathbf{K}^{-1}\mathbf{M}}\,\tan^{-1}\frac{\sqrt{\mathbf{M}^{-1}\mathbf{K}}}{\pi}\Big]\dot{\mathbf{q}} + \mathbf{K}\mathbf{q} = \mathbf{0}\end{aligned} \tag{12}$$

possesses classical normal modes. Numerical values of $\mathbf{M}$ and $\mathbf{K}$ matrices are assumed to be the same as in example 1.

Direct calculation shows

$$\mathbf{C} = -\begin{bmatrix} 67.9188 & 104.8208 & 95.9566 \\ 104.8208 & 161.1897 & 147.7378 \\ 95.9566 & 147.7378 & 135.2643 \end{bmatrix}. \tag{13}$$

Using the modal matrix calculated before in equation (4), we obtain

$$\mathbf{\Phi}^T\mathbf{C}\mathbf{\Phi} = \begin{bmatrix} -88.9682 & 0.0 & 0.0 \\ 0.0 & 0.0748 & 0.0 \\ 0.0 & 0.0 & 0.5293 \end{bmatrix},$$

a diagonal matrix. Analytically the modal damping factors can be obtained as

$$2\zeta_j\omega_j = e^{-\omega_j^4/2}\sinh\left(\frac{1}{\omega_j^2}\ln\frac{4}{3}\omega_j\right) + \omega_j^2\cos^2\left(\frac{1}{\omega_j^2}\right)\frac{1}{\sqrt{\omega_j}}\tan^{-1}\frac{\omega_j}{\pi} \tag{14}$$

where ω_j are the undamped natural frequencies of the system.

This example shows that using the generalized proportional damping it is possible to model any variation of the damping factors with respect to the frequency. This is the basis of the damping identification method to be proposed later in the paper. With Rayleigh's proportional damping in equation (1), the modal damping factors have a special form

$$\zeta_j = \frac{1}{2}\left(\frac{\alpha_1}{\omega_j} + \alpha_2\omega_j\right). \tag{15}$$

Clearly, not all form of variations of ζ_j with respect to ω_j can be captured using equation (15). The damping identification method proposed in the next section removes this restriction.

DAMPING IDENTIFICATION USING GENERALIZED PROPORTIONAL DAMPING

Derivation of the identification method

The damping identification method is based on the expressions of the proportional damping matrix given in theorem 2. Considering expression (a) in theorem 2 it can be shown that (see the Appendix for details)

$$\begin{aligned} \mathbf{\Phi}^T\mathbf{C}\mathbf{\Phi} &= \beta_1\left(\mathbf{\Omega}^2\right) + \mathbf{\Omega}^2\beta_2\left(\mathbf{\Omega}^{-2}\right) \\ \text{or} \quad 2\boldsymbol{\zeta}\,\mathbf{\Omega} &= \beta_1\left(\mathbf{\Omega}^2\right) + \mathbf{\Omega}^2\beta_2\left(\mathbf{\Omega}^{-2}\right). \end{aligned} \tag{16}$$

The modal damping factors can be expressed from equation (16) as

$$\zeta_j = \frac{1}{2}\frac{\beta_1(\omega_j^2)}{\omega_j} + \frac{1}{2}\omega_j\beta_2\left(1/\omega_j^2\right). \tag{17}$$

For the purpose of damping identification the function β_2 can be omitted without any loss of generality. To simplify the identification procedure, the damping matrix is expressed by

$$\mathbf{C} = \mathbf{M}f\left(\mathbf{M}^{-1}\mathbf{K}\right). \tag{18}$$

Using this simplified expression, the modal damping factors can be obtained as

$$2\zeta_j\omega_j = f\left(\omega_j^2\right) \tag{19}$$

$$\text{or} \quad \zeta_j = \frac{1}{2\omega_j}f\left(\omega_j^2\right) = \widehat{f}(\omega_j) \quad \text{(say)}. \tag{20}$$

The function $\widehat{f}(\bullet)$ can be obtained by fitting a continuous function representing the variation of the measured modal damping factors with respect to the natural frequencies. From equations (18) and (19) note that in the argument of $f(\bullet)$, the term ω_j can be replaced by $\sqrt{\mathbf{M}^{-1}\mathbf{K}}$ while obtaining the damping matrix. With the fitted function $\widehat{f}(\bullet)$, the damping matrix can be identified using equation (20) as

$$2\zeta_j\omega_j = 2\omega_j\widehat{f}(\omega_j) \tag{21}$$

$$\text{or} \quad \widehat{\mathbf{C}} = 2\mathbf{M}\sqrt{\mathbf{M}^{-1}\mathbf{K}}\;\widehat{f}\left(\sqrt{\mathbf{M}^{-1}\mathbf{K}}\right). \tag{22}$$

The following example will clarify the identification procedure.

Example 4.

Suppose figure 1 shows modal damping factors as a function of frequency obtained by conducting simple vibration testing on a structure. The damping factors are such that, within the frequency range considered, they show very low values in the low frequency region, high values in the mid frequency region and again low values in the high frequency region. We want to identify a damping model which shows this kind of behavior. The first step is to identify the function which produces this curve. Here this (continuous) curve was simulated using the equation

$$\widehat{f}(\omega) = \frac{1}{15}\left(e^{-2.0\omega} - e^{-3.5\omega}\right)\left(1 + 1.25\sin\frac{\omega}{7\pi}\right)\left(1 + 0.75\omega^3\right). \tag{23}$$

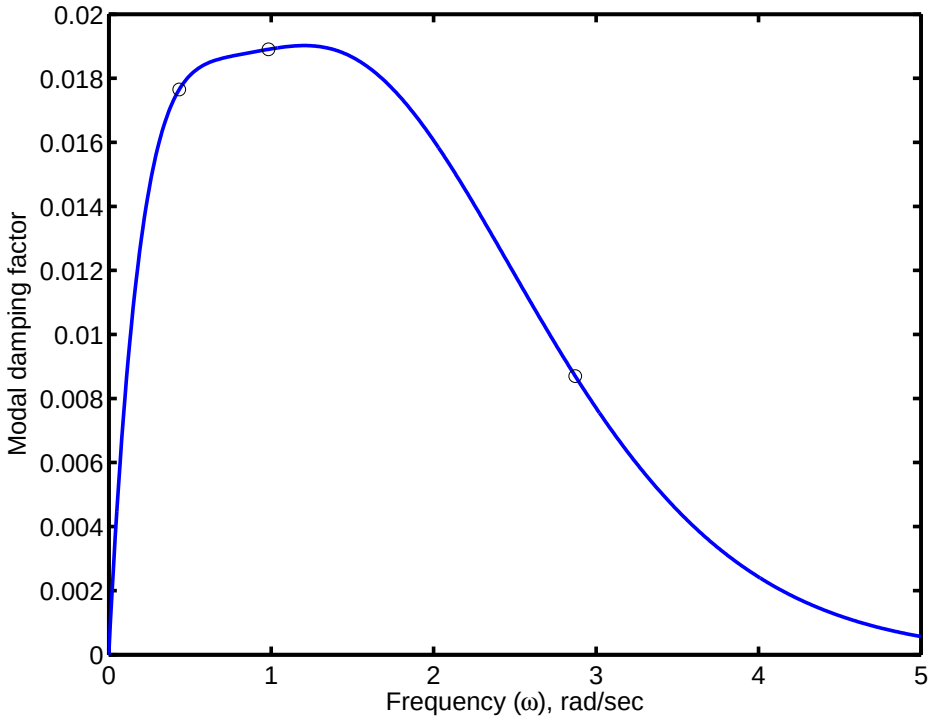

Figure 1: Variation of modal damping factors; —- original, ∘ recalculated.

From the above equation, the modal damping factors in terms of the discrete natural frequencies, can be obtained by

$$2\xi_j\omega_j = \frac{2\omega_j}{15}\left(e^{-2.0\omega_j} - e^{-3.5\omega_j}\right)\left(1 + 1.25\sin\frac{\omega_j}{7\pi}\right)\left(1 + 0.75\omega_j^3\right). \tag{24}$$

To obtain the damping matrix, consider equation (24) as a function of ω_j^2 and replace ω_j^2 by $\mathbf{M}^{-1}\mathbf{K}$ (that is ω_j by $\sqrt{\mathbf{M}^{-1}\mathbf{K}}$) and any constant terms by that constant times $\mathbf{I}$. Therefore, from equation (24) we have

$$\begin{aligned}\mathbf{C} =& \mathbf{M}\,\frac{2}{15}\sqrt{\mathbf{M}^{-1}\mathbf{K}}\left[e^{-2.0\sqrt{\mathbf{M}^{-1}\mathbf{K}}} - e^{-3.5\sqrt{\mathbf{M}^{-1}\mathbf{K}}}\right] \\ &\times\left[\mathbf{I} + 1.25\sin\left(\frac{1}{7\pi}\sqrt{\mathbf{M}^{-1}\mathbf{K}}\right)\right]\left[\mathbf{I} + 0.75(\mathbf{M}^{-1}\mathbf{K})^{3/2}\right]\end{aligned} \tag{25}$$

as the identified damping matrix. Using the numerical values of $\mathbf{M}$ and $\mathbf{K}$ from example 1 we obtain

$$\mathbf{C} = \begin{bmatrix} 2.3323 & 0.9597 & 1.4255 \\ 0.9597 & 3.5926 & 3.7624 \\ 1.4255 & 3.7624 & 7.8394 \end{bmatrix} \times 10^{-2}. \tag{26}$$

If we recalculate the damping factors from the above constructed damping matrix, it will produce three points corresponding to the three natural frequencies which will exactly match with our initial curve as shown in figure 1.

The method outlined here can produce accurate damping matrix if the modal damping factors are known. All polynomial fitting methods can be employed to approximate $\widehat{f}(\omega)$ and one can construct a damping matrix corresponding to the fitted function by the procedure outlined here. As an example, if $2\xi_j\omega_j$ can be represented in a Fourier series

$$2\xi_j\omega_j = \frac{a_0}{2} + \sum_{r=1}^{\infty}\left[a_r\cos\left(\frac{2\pi r\omega_j}{\Omega}\right) + b_r\sin\left(\frac{2\pi r\omega_j}{\Omega}\right)\right] \tag{27}$$

then the damping matrix can also be expanded in a Fourier series as

$$\mathbf{C} = \mathbf{M}\left(\frac{a_0}{2}\mathbf{I} + \sum_{r=1}^{\infty}\left[a_r \cos\left(2\pi r\Omega^{-1}\sqrt{\mathbf{M}^{-1}\mathbf{K}}\right) + b_r \sin\left(2\pi r\Omega^{-1}\sqrt{\mathbf{M}^{-1}\mathbf{K}}\right)\right]\right). \tag{28}$$

The damping identification procedure itself does not introduce significant errors as long as the modes are not highly complex. From equation (22) it is obvious that the accuracy of the fitted damping matrix depends heavily on the accuracy the mass and stiffness matrix models. In summary, this identification procedure can be described by the following steps:

1. Measure a suitable transfer function $H_{ij}(\omega)$ by conducting vibration testing.
2. Obtain the undamped natural frequencies ω_j and modal damping factors ζ_j, for example, using the circle-fitting method.
3. Fit a function $\zeta = \widehat{f}(\omega) : \mathbb{R}^+ \rightarrow \mathbb{R}^+$ which represents the variation of ζ_j with respect to ω_j for the range of frequency considered in the study.
4. Calculate the temporary matrix
$$\mathbf{T} = \sqrt{\mathbf{M}^{-1}\mathbf{K}} \tag{29}$$
5. Obtain the damping matrix using
$$\widehat{\mathbf{C}} = 2\,\mathbf{M}\,\mathbf{T}\,\widehat{f}\,(\mathbf{T}) \tag{30}$$

Most of the currently available finite element based modal analysis packages usually offer Rayleigh's proportional damping model and a constant (frequency independent) damping factor model. A generalized proportional damping model together with the proposed damping identification technique can be easily incorporated within the existing tools to enhance their damping modelling capabilities without using significant additional resources.

Comparison with the existing methods

The proposed method is by no means the only approach to obtain the damping matrix within the scope of proportional damping assumption. Géradin and Rixen (1997) have outlined a systematic method to obtain the damping matrix using Caughey series (6). The coefficients α_j in series (6) can be obtained by solving the linear system of equations

$$\mathbf{W}\boldsymbol{\alpha} = \boldsymbol{\zeta}_v \tag{31}$$

where

$$\mathbf{W} = \frac{1}{2}\begin{bmatrix} \frac{1}{\omega_1} & \omega_1 & \omega_1^3 & \cdots \omega_1^{2N-3} \\ \frac{1}{\omega_2} & \omega_2 & \omega_2^3 & \cdots \omega_2^{2N-3} \\ \vdots & \vdots & \vdots & \vdots \\ \frac{1}{\omega_N} & \omega_N & \omega_N^3 & \cdots \omega_N^{2N-3} \end{bmatrix}, \quad \boldsymbol{\alpha} = \begin{Bmatrix} \alpha_1 \\ \alpha_2 \\ \vdots \\ \alpha_N \end{Bmatrix} \quad \text{and} \quad \boldsymbol{\zeta}_v = \begin{Bmatrix} \zeta_1 \\ \zeta_2 \\ \vdots \\ \zeta_N \end{Bmatrix}. \tag{32}$$

The mass and stiffness matrices and the constants α_j calculated from the preceding equation can be substituted in equation (6) to obtain the damping matrix. Géradin and Rixen (1997) have mentioned that the coefficient matrix $\mathbf{W}$ in (32) becomes ill-conditioned for systems with well separated natural frequencies.

Another simple, yet very general, method to obtain the proportional damping matrix is by using the inverse modal transformation method. Adhikari and Woodhouse (2001a) have also used this approach in the context of identification of non-proportionally damped systems. From experimentally obtained modal damping factors and natural frequencies one can construct the diagonal modal damping matrix $\mathbf{C}' = \boldsymbol{\Phi}^T\mathbf{C}\boldsymbol{\Phi}$ as

$$\mathbf{C}' = 2\boldsymbol{\zeta}\boldsymbol{\Omega}. \tag{33}$$

From this, the damping matrix in the original coordinate can be obtained using the inverse transformation as

$$\mathbf{C} = \boldsymbol{\Phi}^{-T}\mathbf{C}'\boldsymbol{\Phi}^{-1}. \tag{34}$$

The damping matrix identification using equation (34) is essentially numerical in nature. In that it is difficult to visualize any underlying structure of the modal damping factors of a particular system. With the proposed method it is possible to identify the proportional damping functions corresponding to several standard components such as damped beams, plates and shells, and investigate if there are any inherent functional forms associated with them. It will be particularly useful if one can identify typical functional forms of modal damping factors associated with different structural components.

For a given structure, if the degrees-of-freedom of the finite element (FE) model and experimental model (that is the number of sensors and actuators) are the same, equation (34) and the proposed method would yield similar damping matrices. Usually the numerical model of a structure has more degrees-of-freedom compared to the degrees-of-freedom of the experimental model. With the conventional modal identification method it is also difficult to accurately estimate the modal parameters (natural frequencies and damping factors) beyond the first few modes. Suppose the numerical model has dimension N and we have measured the modal parameters of first $n < N$ number of modes. The dimension of $\mathbf{C}'$ in equation (33) will be $n \times n$ whereas for further numerical analysis using FE method we need the $\mathbf{C}$ matrix to be of dimension $N \times N$. This implies that there is a need to extrapolate the available information. If the modal matrix from an FE model is used, one way this can be achieved is by using a $N \times n$ rectangular $\mathbf{\Phi}$ matrix in equation (34), where the n columns of $\mathbf{\Phi}$ would consist of the mode shapes corresponding to the measured modes. Since $\mathbf{\Phi}$ becomes a rectangular matrix, a pseudo-inverse is required to calculate $\mathbf{\Phi}^{-T}$ and $\mathbf{\Phi}^{-1}$ in equation (34). Because pseudo-inverse of a matrix essentially arises from a least-square error minimization, it would introduce unquantified errors in the modal damping factors associated with the higher modes (which have not been measured). The proposed method handles this situation in a natural way. Since a continuous function has been fitted to the measured damping factors, the method would preserve the functional trend to the higher modes for which the modal parameters have not been measured. This property of the proposed identification method is particularly useful provided the modal damping factors of the structure under investigation do not show significantly different behavior in the higher modes. These issues are clarified in the following example.

Example 5.

A partly damped linear array of spring-mass oscillator is considered to illustrate the application of proposed damping identification method. The objective of this study is to compare the performance of the proposed method with existing methods. The system, together with the numerical values assumed for different parameters are shown in figure 2. The mass matrix of the system has the form $\mathbf{M} = m\mathbf{I}$ where $\mathbf{I}$ is the $N \times N$

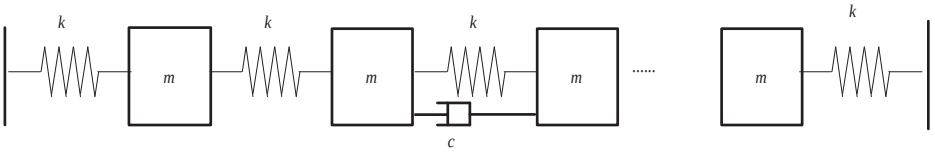

Figure 2: Linear array of N spring-mass oscillators, $N = 30$, $m = 1$ kg, $k = 3.95 \times 10^5$ N/m. Dampers are attached between 8th and 23rd masses with $c = 40$ Ns/m.

identity matrix. The stiffness matrix of the system is given by

$$\mathbf{K} = k \begin{bmatrix} 2 & -1 & & & & & \\ -1 & 2 & -1 & & & & \\ & \ddots & \ddots & \ddots & & & \\ & & -1 & 2 & -1 & & \\ & & & \ddots & \ddots & -1 & \\ & & & & -1 & 2 & \end{bmatrix}. \tag{35}$$

Some of the masses of the system shown in figure 2 have viscous dampers connecting them to each other. The damping matrix $\mathbf{C}$ has similar form to the stiffness matrix except that it has non-zero entries corresponding to the masses attached with the dampers only. With such a damping matrix it is easy to verify that the system is actually non-proportionally damped. For numerical calculations, we have considered a thirty-degree-of-freedom system so that $N = 30$. Values of the mass and stiffness associated with each unit are

assumed to be the same with numerical values of $m = 1$ kg and $k = 3.95 \times 10^5$ N/m. The resulting undamped natural frequencies then range from approximately 10 to 200 Hz. The value $c = 40$ Ns/m has been used for the viscous damping coefficient of the dampers.

We consider a realistic situation where the modal parameters of only first ten modes are known. Numerical values of ω_j and ζ_j for the first ten modes are shown in table 1. Because the system is non-proportionally damped, the complex eigensolutions are obtained using the state-space analysis (Newland, 1989) and the modal damping factors are calculated from the complex eigenvalues as $\zeta_j = -\text{Re}(\lambda_j)/|\text{Im}(\lambda_j)|$. Using this

Table 1: Natural frequencies (Hz) and modal damping factors for first ten modes

Modes:	1	2	3	4	5	6	7	8	9	10
Natural frequencies	10.1326	20.2392	30.2938	40.2707	50.1442	59.8890	69.4800	78.8927	88.1029	97.0869
Damping factors	0.0005	0.0032	0.0057	0.0060	0.0067	0.0095	0.0117	0.0117	0.0125	0.0155

data, the following three methods are used to fit a proportional damping model:

(a) method using Caughey series

(b) inverse modal transformation method

(c) the method using generalized proportional damping

The modal damping factors corresponding to the higher modes, that is from mode number 11 to 30, are available from simulation results. The aim of this example is to see how the modal damping factors obtained using the identified damping matrices from the above three methods compare with the 'true' modal damping factors corresponding to the higher modes.

For the method using Caughey series, it has not been possible to obtain the constants α_j from equation (31) since the associated $\mathbf{W}$ matrix become highly ill-conditioned. Numerical calculation shows that the 10×10 matrix $\mathbf{W}$ has a condition number of 1.08×10^{51}. To apply the inverse modal transformation method, only the first ten columns of the analytical modal matrix $\mathbf{\Phi}$ are retained in the truncated modal matrix $\widehat{\mathbf{\Phi}} \in \mathbb{R}^{30\times 10}$. Using the pseudo inverse, the damping matrix in the original coordinate has been obtained from equation (34) as

$$\mathbf{C} = \left[\left(\widehat{\mathbf{\Phi}}^T\widehat{\mathbf{\Phi}}\right)^{-1}\widehat{\mathbf{\Phi}}^T\right]^T [2\boldsymbol{\zeta}\mathbf{\Omega}] \left[\left(\widehat{\mathbf{\Phi}}^T\widehat{\mathbf{\Phi}}\right)^{-1}\widehat{\mathbf{\Phi}}^T\right]. \tag{36}$$

From the identified $\mathbf{C}$ matrix, the modal damping factors are recalculated using

$$\boldsymbol{\zeta} = \frac{1}{2}[\mathbf{\Phi}^T\mathbf{C}\mathbf{\Phi}]\mathbf{\Omega}^{-1} \tag{37}$$

where $\mathbf{\Phi}$ is the full 30×30 modal matrix.

Now consider the proposed method using generalized proportional damping. Using the data in table 1, figure 3 shows the variation of modal damping factors for first the ten modes. Looking at the pattern of the curve in figure 3 we have selected the function $\widehat{f}(\bullet)$ as

$$\zeta = \widehat{f}(\omega) = \theta_1\omega + \theta_2 \sin(\theta_3\omega) \tag{38}$$

where $\theta_i, i = 1, 2, 3$ are undetermined constants. Using the data in table 1, together with a nonlinear least-square error minimization approach results

$$\theta_1 = 0.0245 \times 10^{-3} \quad \text{and} \quad \theta_2 = -0.5622 \times 10^{-3} \quad \text{and} \quad \theta_3 = 9.0. \tag{39}$$

Recalculated values of ζ_j using this fitted function is compared with the original function in figure 3. This simple function matches well with the original modal data. Note that neither the function in equation (38), nor the parameter values in equation (39) are unique. One can use more complex functions and sophisticated parameter fitting procedures to obtain more accurate results.

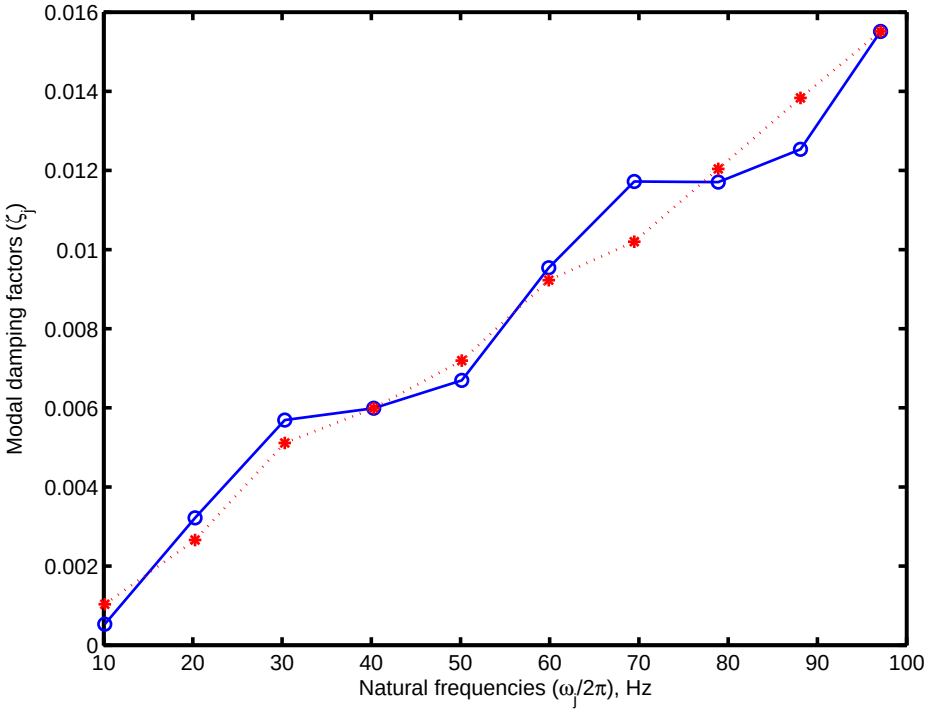

Figure 3: Modal damping factors for first ten modes; –○– original, ···∗··· fitted generalized proportional damping function.

The damping matrix corresponding to the fitted function in equation (38) can be obtained using equation (22) as

$$\begin{aligned}\mathbf{C} &= 2\mathbf{M}\sqrt{\mathbf{M}^{-1}\mathbf{K}}\,\widehat{f}\left(\sqrt{\mathbf{M}^{-1}\mathbf{K}}\right)\\ &= 2\mathbf{M}\sqrt{\mathbf{M}^{-1}\mathbf{K}}\left[\theta_1\sqrt{\mathbf{M}^{-1}\mathbf{K}}+\theta_2\sin\left(\theta_3\sqrt{\mathbf{M}^{-1}\mathbf{K}}\right)\right]\\ &= 2\theta_1\,\mathbf{K}+2\theta_2\,\mathbf{M}\sqrt{\mathbf{M}^{-1}\mathbf{K}}\,\sin\left(\theta_3\sqrt{\mathbf{M}^{-1}\mathbf{K}}\right)\end{aligned} \tag{40}$$

The first part of the $\mathbf{C}$ matrix in equation (40) is stiffness proportional and the second part is mass proportional in the sense of generalized proportional damping.

As mentioned earlier, the aim of this study is to see how the different methods work when modal damping factors are compared against full set of 30 modes. In figure 4, the values of ζ_j obtained by the inverse modal transformation method in equation (37) is compared with the original damping factors for all the 30 modes calculated using complex modal analysis. As expected, there is a perfect match with the original damping factors for the first ten modes. However, beyond the first ten modes the damping factors obtained using the inverse modal transformation method do not match with the true damping factors. This is also expected since this information has not been used in equations (36) and (37) and the method itself is not capable of extrapolating the available modal information. Modal damping factors using the fitted function in equation (38) are also shown in figure 4 for all 30 modes. The 'predicted' damping factors for modes 11 to 30 matched well with the original modal damping factors. This is due to the fact that the pattern of the variation of modal damping factors with natural frequencies does not change significantly beyond the first ten modes and hence the fitted function provides a good description of the variation. This study demonstrates the advantage of using generalized proportional damping over the conventional proportional damping models.

DAMPING MODELLING OF COMPLEX SYSTEMS

The method proposed in the previous section is ideally suitable for small structures for which 'global' measurements can be obtained. For a large complex structure such as an aircraft, neither the global vibration measurements, nor the processing of global mass and stiffness matrices in the manner described before are

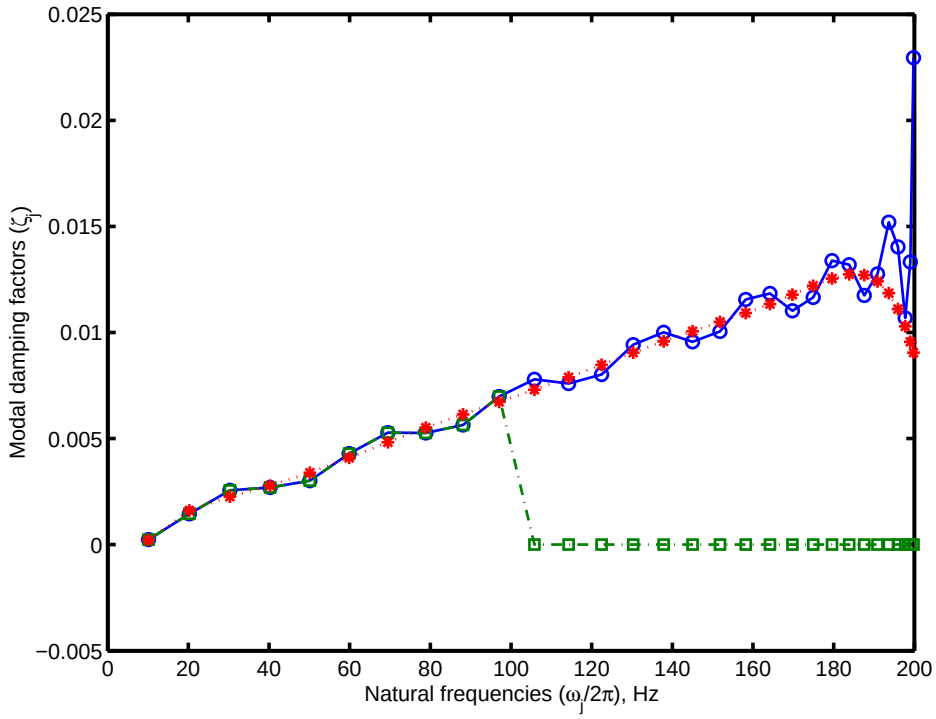

Figure 4: Modal damping factors for all 30 modes; $-\circ-$ original, $.\text{-}\square.\text{-}$. fitted using inverse modal transformation, $\cdots * \cdots$ fitted usiing generalized proportional damping.

straightforward. However, it is possible to identify the generalized proportional damping models for different components or substructures chosen suitably. For example, to model the damping of an aircraft fuselage one could fit generalized proportional damping models for all the ribs and panels by testing them separately and then combine the element (or substructure) damping matrices in a way similar to the assembly of the mass and stiffness matrices in the standard finite element method. The overall damping modelling procedure can be described as follows:

1. Divide a structure into m elements/substructures suitable for individual vibration testing.
2. Measure a transfer function $H_{ij}^{(e)}(\omega)$ by conducting vibration testing of e-th element/substructure.
3. Obtain the undamped natural frequencies $\omega_j^{(e)}$ and modal damping factors $\zeta_j^{(e)}$ for e-th element/substructure.
4. Fit a function $\zeta_{(e)} = \widehat{f}_{(e)}(\omega)$ which represents the variation of damping factors with respect to frequency for the e-th element/substructure.
5. Calculate the matrix $\mathbf{T}_{(e)} = \sqrt{\mathbf{M}_{(e)}^{-1}\mathbf{K}_{(e)}}$
6. Obtain the element/substructure damping matrix using the fitted proportional damping function as $\widehat{\mathbf{C}}_{(e)} = 2\,\mathbf{M}_{(e)}\mathbf{T}_{(e)}\widehat{f}_{(e)}\left(\mathbf{T}_{(e)}\right)$
7. Repeat the steps from 2 to 6 for all $e = 1, 2, \cdots, m$.
8. Obtain the global damping matrix as $\widehat{\mathbf{C}} = \sum_{e=1}^{m} \widehat{\mathbf{C}}_{(e)}$. Here the summatation is over the relevant degrees-or-freedom as in the standard finite element method.

It is anticipated that the above procedure would result in a more realistic damping matrix compared to simply using the damping factors arising from global vibration measurements. Using this approach, the damping matrix will be proportional only within an element/substructure level. After the assembly of the elementt/substructure matrices, the global damping matrix will in general be non-proportional. Experimental and numerical works are currently in progress to test this method for large systems.

EXPERIMENTAL STUDIES

Damping identification in a free-free beam

System model and experimental methodology

A steel beam with uniform rectangular cross-section is considered for the experiment. The physical and geometrical properties of the steel beam are shown in Table 2. For the purpose of this experiment a double sided glued tape is sandwiched between the beam and a thin aluminum plate. This arrangement is similar to a constrained layer damping (Ungar, 2000). The impulse is applied at 11 uniformly spaced locations on the

Table 2: Material and geometric properties of the beam considered for the experiment

Beam Properties	Numerical values
Length (L)	1.00 m
Width (b)	39.0 mm
Thickness (t_h)	5.93 mm
Mass density (ρ)	7800 Kg/m^3
Youngs modulus (E)	2.0×10^5 GPa
Cross sectional area ($a = bt_h$)	2.3127×10^{-4} m^2
Moment of inertia ($I = 1/12bt_h^3$)	6.7772×10^{-10} m^4
Mass per unit length (ρ_l)	1.8039 Kg/m
Bending rigidity (EI)	135.5431 Nm^2

beam. We have tried to simulate the free-free condition for the beam by hanging it using two strings. The two string arrangement for suspending the beam is found to reduce torsional modes. A schematic diagram of the experimental set-up is shown in figure 5.

The vibration response of the beam is measured using the Polytec^{TM} laser vibrometer. The laser beam, which is targeted at a selected measurement point on the test structure, is reflected and interferes with a reference beam inside the scanning head. Since the surface of the test structure is moving in space with a varying velocity due to vibrations, the reflected laser beam will have a frequency which is different from that of the reference beam. This is due to the well known Doppler effect. Measuring this shift in frequency permits the determination of the velocity component of the surface in a direction parallel to the laser beam. The interfered light is processed by the vibrometer controller, which generates an *analogue* voltage signal that is proportional to the surface target velocity in the direction parallel to the emitted laser beam. By sampling a reference signal the laser scanner can be triggered by an external excitation source signal such as an impulse hammer signal. The excitation and laser measurement signals are fed to a PC with independent data logging ability.

The Polytec^{TM} vibrometer software allows one to choose the data acquisition settings such as the sampling frequency, vibrometer sensitivity scale, filters, window functions *etc.*. The in-house data logging software is used to process the measured signals. This software has the capability to log time series, calculate spectra, and perform modal analysis and curve fitting to extract natural frequencies and mode shapes.

Results and discussions

Results from the initial testing on the 'undamped beam', that is without the damping mechanism, showed that damping is extremely light. This ensures that the significant part of the damping comes from the localized constrained damping layer only. Measured natural frequencies, damping factors and natural frequencies obtained from the finite element (FE) method for the first eleven modes are shown in Table 3. Timoshenko bending beam elements were used for the finite element (FE) model. The degrees-of-freedom of the FE model (N) used in this study is 90 and the associated FE mesh is shown in Figure 6. Percentage errors in the natural frequencies obtained from the finite element method with respect to the experimental methods are also shown in Table 3.

From the first two columns of this table we fit a continuous function. Figure 7 shows the variation of modal damping factors for the first eleven modes. Looking at the pattern of the curve in figure 7 we have selected the function $\widehat{f}(\bullet)$ as

$$\zeta = \widehat{f}(\omega) = a_0 + \left(a_1\omega^{-1} + a_2\omega^{-2} + a_3\omega^{-3}\right) + a_4 \exp\left\{-a_5(\omega - a_6)^2\right\} \tag{41}$$

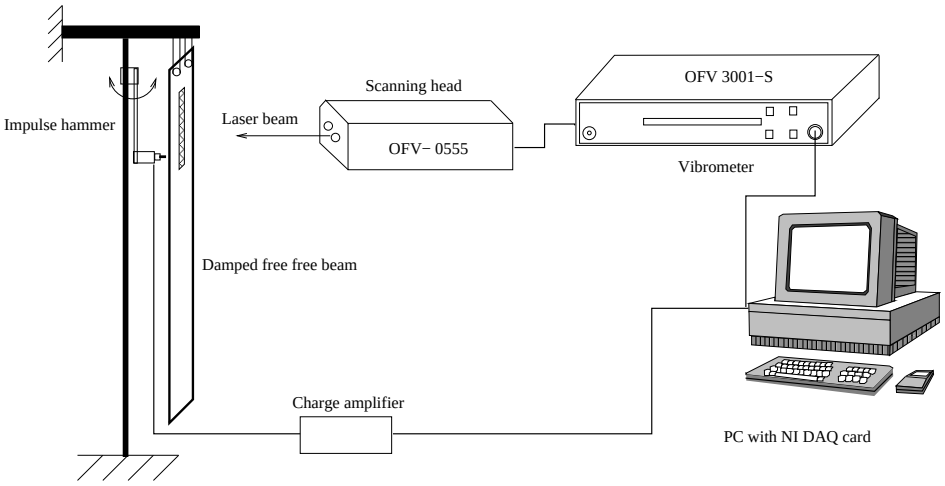

Figure 5: Schematic representation of the experimental set-up of the free-free beam.

Table 3: Measured natural frequencies, damping factors and natural frequencies obtained from the finite element (FE) method of the free-free beam for the first eleven modes (the numbers in the parenthesis correspond to the percentage error with respect to the experimental result)

Natural frequencies, Hz (experimental)	Damping factors (in % of critical damping)	Natural frequencies, Hz (from FE)
33.00	0.6250	30.81 (-6.64 %)
85.00	0.2000	85.24 (0.29 %)
166.00	0.0833	167.61 (0.97 %)
276.00	0.0313	277.73 (0.63 %)
409.00	0.0625	415.67 (1.63 %)
569.00	0.1250	581.42 (2.18 %)
758.00	0.1163	774.94 (2.24 %)
976.00	0.1786	996.20 (2.07 %)
1217.00	0.8621	1245.15 (2.31 %)
1498.00	0.7143	1521.77 (1.59 %)
1750.00	0.3571	1826.06 (4.35 %)

Figure 6: Schematic representation of the Finite element mesh of the of the free-free beam shown in figure 5.

where $a_i, i = 1, \cdots, 6$ are undetermined constants. Using the data in Table 3, together with a nonlinear least-square error minimization approach, the fitted parameters are found to be:

$$\begin{aligned} a_0 = 0.0031, \quad a_1 = -6.26, \quad a_2 = 4.01 \times 10^3, \quad a_3 = -5.18 \times 10^5, \\ a_4 = 0.0079, \quad a_5 = 6.96 \times 10^{-7} \quad \text{and} \quad a_6 = 8.4 \times 10^3. \end{aligned} \tag{42}$$

Recalculated values of ζ_j using this fitted function is compared with the original function in figure 7. This function (the dotted line) matches well with the original modal data. We have also plotted the $\widehat{f}(\omega)$ in (41) as functions of the natural frequencies from experimental measurement and FE in figure 7. Both plots are reasonably close because the difference between the measured and FE natural frequencies are small in this case. Note that neither the function in Eq. (41), nor the parameter values in Eq. (42) are unique. One can use more complex functions and sophisticated parameter fitting procedures to obtain more accurate results.

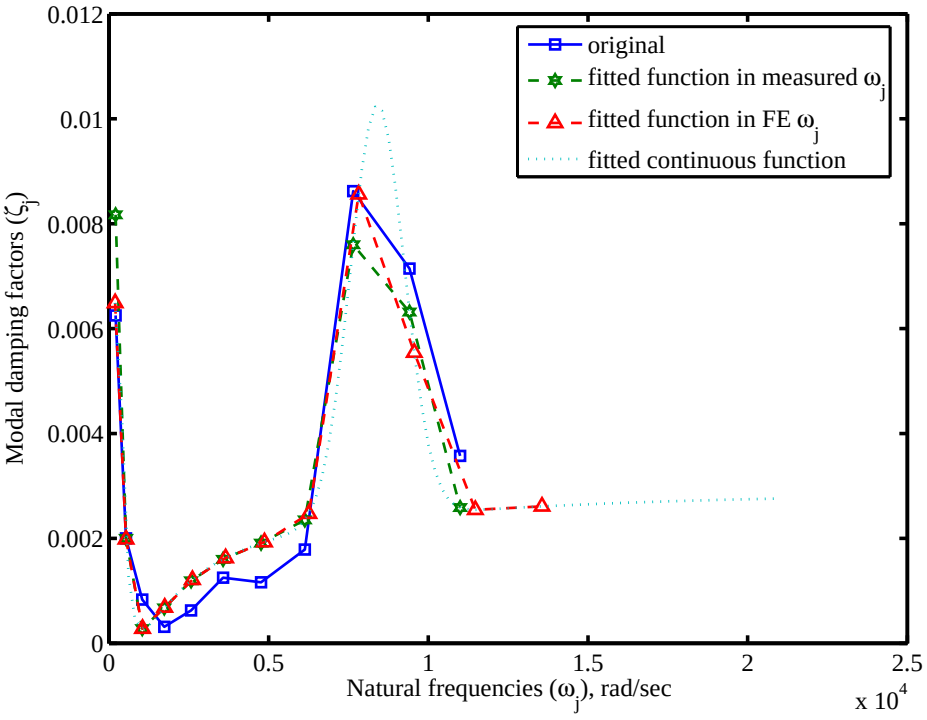

Figure 7: Modal damping factors and fitted generalized proportional damping function for the first eleven modes.

Now that the function $\widehat{f}(\omega)$ has been identified, the next step is to substitute the 90×90 FE mass and stiffness matrices in Eq. (22) (or equivalently in Eq. (30)) to obtain the damping matrix. For this example we have

$$\begin{aligned}\widehat{\mathbf{C}} &= 2\mathbf{M}\mathbf{T}\left[a_0\mathbf{I} + \left(a_1\mathbf{T}^{-1} + a_2\mathbf{T}^{-2} + a_3\mathbf{T}^{-3}\right) + a_4\exp\left\{-a_5\left(\mathbf{T} - a_6\mathbf{I}\right)^2\right\}\right] \in \mathbb{R}^{90\times 90} \\ &= 2\left(a_1\mathbf{M} + a_3\mathbf{K}\right) + 2\mathbf{M}\sqrt{\mathbf{M}^{-1}\mathbf{K}}\left[a_0\mathbf{I} + a_2\mathbf{K}^{-1}\mathbf{M} + a_4\exp\left\{-a_5\left(\sqrt{\mathbf{M}^{-1}\mathbf{K}} - a_6\mathbf{I}\right)^2\right\}\right].\end{aligned} \tag{43}$$

Interestingly, the first part of the $\widehat{\mathbf{C}}$ matrix in Eq. (43) is the classical Rayleigh damping while the second part is mass proportional in the sense of generalized proportional damping. The second part can be viewed as the correction needed to the Rayleigh damping model for the measured data set. Here we have compared our damping identification method with the four methods described before. The modal damping factors obtained using the proposed generalized proportional damping matrix in Eq. (43) is shown in figure 8. In the same plot the results obtained from the other methods are also shown. In order to apply the inverse modal transformation method, only the first eleven columns of the analytical modal matrix are retained to obtain the truncated modal matrix $\widehat{\mathbf{\Phi}} \in \mathbb{R}^{90\times 11}$. This approach reproduces the damping factors for the first eleven modes very accurately. However, beyond the first eleven modes the damping factors obtained using the inverse modal transformation method is just zero (that is effectively all the modes become undamped). The best fitted Rayleigh damping matrix for this example is obtained as

$$\widehat{\mathbf{C}}_b = 2.28\mathbf{M} + 1.06 \times 10^{-6}\mathbf{K}. \tag{44}$$

It was not possible to obtain the constants α_j from Eq. (31) using Caughey method because the associated $\mathbf{W}$ matrix became highly ill-conditioned. For the polynomial fit method, only a second order polynomial could be fitted to avoid the ill-conditioning problem. The best fitted second-order polynomial in this case turns out to be

$$\zeta = p_1 + p_2\omega + p_3\omega^2 \tag{45}$$

where

$$p_1 = 0.00236, \quad p_2 = -2.93 \times 10^{-7} \quad \text{and} \quad p_3 = 6.2 \times 10^{-11}. \tag{46}$$

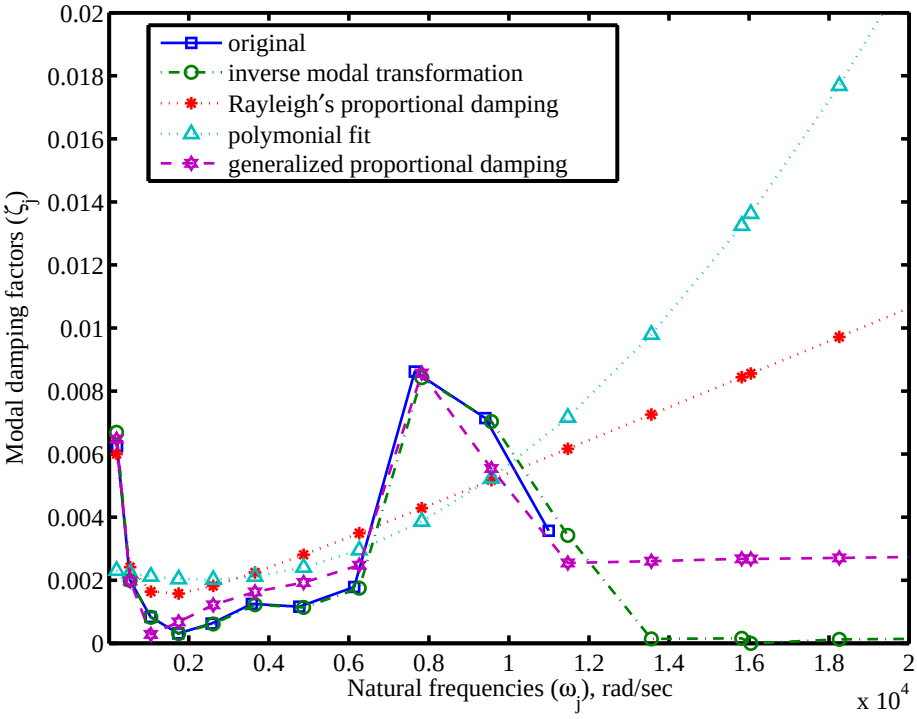

Figure 8: Comparison of modal damping factors using different proportional damping matrix identification method.

The damping matrix corresponding to the polynomial in Eq. (45) can be obtained as

$$\widehat{\mathbf{C}}_d = 2\mathbf{MT}\left[p_1\mathbf{I} + p_2\mathbf{T} + p_3\mathbf{T}^2\right] = 2p_2\mathbf{K} + 2(p_1\mathbf{M} + p_3\mathbf{K})\sqrt{\mathbf{M}^{-1}\mathbf{K}}. \tag{47}$$

This matrix, like the Rayleigh damping matrix, shows high modal damping values beyond the fitted modes.

Damping identification in a clamped plate with slots

System model and experimental methodology

In this section we consider a two dimensional structure. A schematic model of the test structure is shown in figure 9. This is fabricated by making slots in a mild steel rectangular plate of 2 mm thickness, resulting in three cantilever beams joined at their base by a rectangular plate. A schematic diagram of the test rig

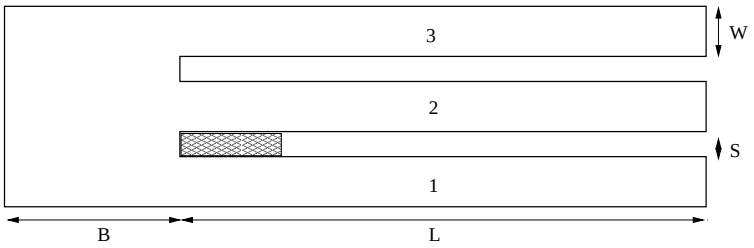

Figure 9: Geometric parameters of the plate with slots: $B = 50mm$, $L = 400mm$, $S = 10mm$, $W = 20mm$. The source of damping in this test structure is the wedged foam between the beams 1 and 2.

is shown in figure 10. The test system is fixed to a heavy table at the root so that the three cantilever-like vanes are free to oscillate. A pendulum type impulse hammer is used to excite each vane of the structure close to the base of each vane. This mechanism delivers the impulse exactly at the same point repeatedly, so that better measurements can be obtained.

The data flow in the experiments is as follows. The impulse hammer signal is passed through a charge amplifier and then fed to the PC data logging system. The vibration response measured by the vibrometer is

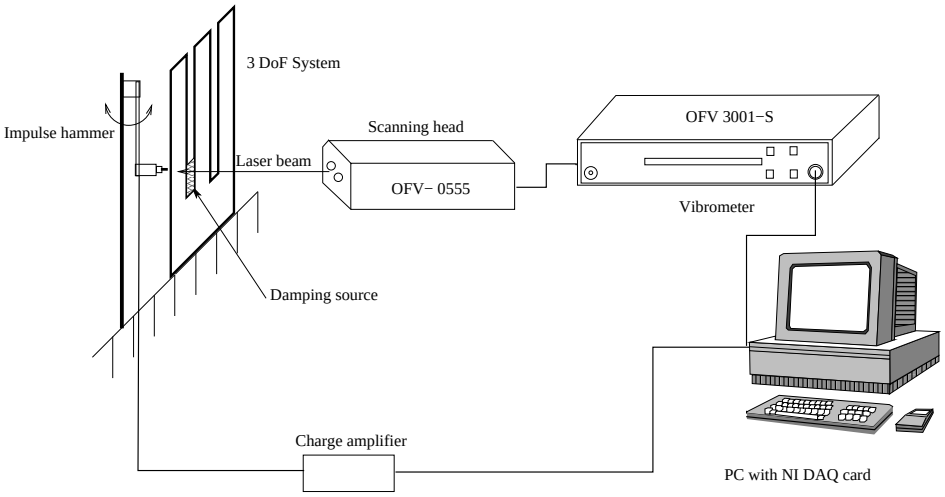

Figure 10: Schematic representation of the experimental set-up of the clamped plate with slots.

also fed to the PC to compute the FRF. The frequency response of this system, shown in figure 11, exhibits characteristic clustering of vibration modes in to bands (Phani, 2004). Notice that the coherence is very close to unity (zero on log scale) till 500 Hz and the data of interest is in the range of 10-300 Hz. Thus a good FRF for each input/output combination was obtained. Also the peaks in each pass band are identifiable and hence modal identification methods can be applied with ease on this data. The mode shapes for the three modes in the second and third band are as shown in figures figure 12 and figure 13 respectively. It

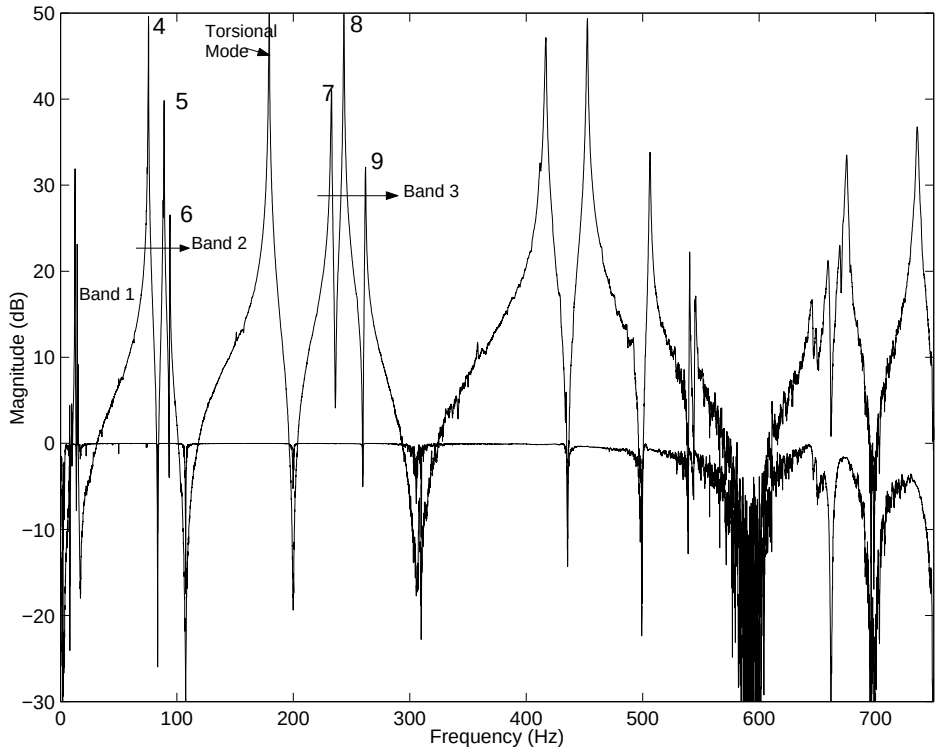

Figure 11: Typical measured FRF on the three cantilever system. Coherence is also shown on the same plot. Each pass band and flexural modes are labelled. Note that the peaks are clearly visible and hence modal identification can be performed with ease.

can be seen that in the second pass band, the cantilever beams deform in the second mode and in the third pass band they deform in the third mode. Thus the approximate mode shapes in each pass band are [1 1

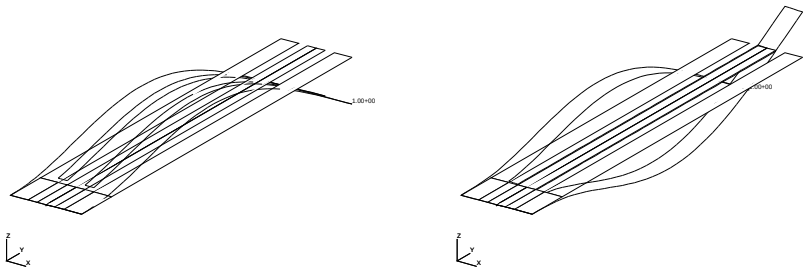

(a) Mode 1, (1, 1, 1)

(b) Mode 2, (1, 0, -1)

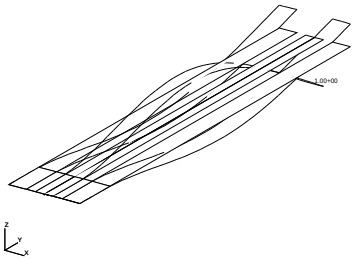

(c) Mode 3, (1, -2, 1)

Figure 12: Mode shapes corresponding to the three modes in the second pass band. It can be noticed that each of the cantilever beams deforms in its second mode in this band. Also notice that the second beam does not deform at all in the second mode of the pass band *i.e.*it is a node.

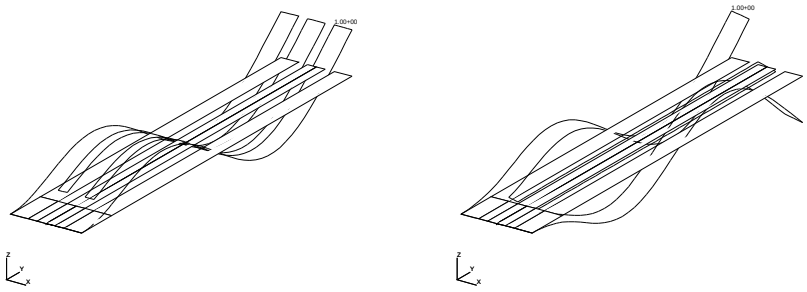

(a) Mode 1, (1, 1, 1)

(b) Mode 2, (1, 0, -1)

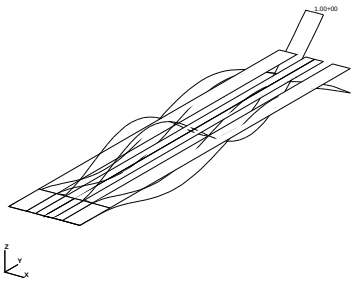

(c) Mode 3, (1, -2, 1)

Figure 13: Mode shapes corresponding to the three modes in the third pass band. It can be noticed that each of the cantilever beams deforms in its third mode in this band. Also notice that the second beam does not deform at all in the second mode of the pass band *i.e.*it is a node.

Table 4: Measured natural frequencies, damping factors and natural frequencies obtained from the finite element (FE) method of the clamped plate with slots for the first nine modes (the numbers in the parenthesis correspond to the percentage error with respect to the experimental result)

Natural frequencies, Hz (experimental)	Damping factors (in % of critical damping)	Natural frequencies, Hz (from FE)
12.46	0.1032	13.14 (5.44 %)
14.36	0.0969	14.45 (0.65 %)
15.01	0.1159	15.08 (0.45 %)
75.60	0.1404	81.32 (7.56 %)
88.94	0.1389	89.68 (0.83 %)
93.97	0.1254	94.49 (0.55 %)
232.74	0.1494	225.95 (-2.92 %)
243.37	0.0953	248.53 (2.12 %)
261.93	0.1260	265.04 (1.19 %)

1], [1 0 -1], and [1 -2 1] based on a particular mode of single cantilever. Furthermore, by *suitably* varying the geometric parameters such as B, L, S and W in figure 9, the modal overlap in each pass band can be controlled.

Results and discussions

The finite element mesh of the test structure is shown in figure 14. Measured natural frequencies, damping

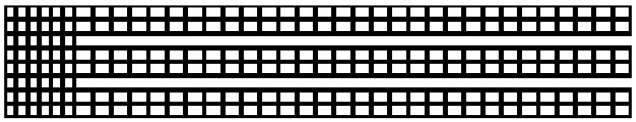

Figure 14: Schematic representation of the Finite element mesh of the of the clamped plate with slots shown in figure 10.

factors and natural frequencies obtained from the finite element (FE) method for the first nine modes are shown in Table 4. Four noded rectangular plate bending elements were used for the finite element (FE) model using ABAQUS/standrad software (Hibbit, Kralson & Soresen, Inc.). The resulting system model has 972 degrees of freedom. Percentage errors in the natural frequencies obtained from the finite element method with respect to the experimental methods are also shown in this table.

From the first two columns of Table 4 we fit a continuous function. Figure 15 shows the variation of modal damping factors for the first nine modes. Looking at the pattern of the curve in figure 15 we have selected the function $\widehat{f}(\bullet)$ as

$$\zeta = \widehat{f}(\omega) = a_0 + a_1 \exp\left\{-a_2(\omega - a_3)^2\right\} + a_4 \exp\left\{-a_5(\omega - a_6)^2\right\} \tag{48}$$

where $a_i, i = 0, \cdots, 6$ are undetermined constants. Using the data in Table 4, together with a nonlinear least-square error minimization approach results

$$\begin{aligned} a_0 = 9.53 \times 10^{-4}, \quad a_1 = 4.51 \times 10^{-4}, \quad a_2 = 2.27 \times 10^{-5}, \quad a_3 = 475, \\ a_4 = 5.41 \times 10^{-4}, \quad a_5 = 3.7 \times 10^{-6}, \quad \text{and} \quad a_6 = 1.46 \times 10^{3}. \end{aligned} \tag{49}$$

Recalculated values of ζ_j using this fitted function is compared with the original function in figure 15. This function (the dotted line) matches well with the original modal data. We have also plotted the $\widehat{f}(\omega)$ in Eq. (38) as functions of the natural frequencies from experimental measurement and FE in figure 15. Both plots are reasonably close because the difference between the measured and FE natural frequencies are small in this case. Again, neither the function in Eq. (48), nor the parameter values in Eq. (49) are unique. One can use more complex functions and sophisticated parameter fitting procedures to obtain more accurate results.

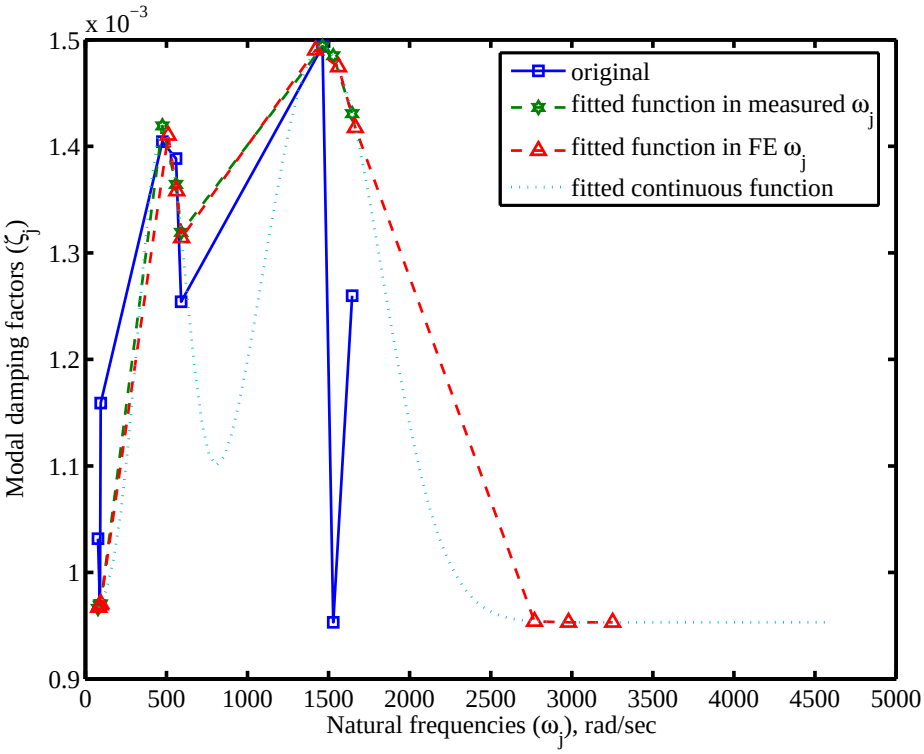

Figure 15: Modal damping factors and fitted generalized proportional damping function for the first nine modes of the clamped plate with slots.

After the identification of the function $\widehat{f}(\omega)$, the next step is to substitute the 972×972 FE mass and stiffness matrices in Eq. (22) (or equivalently in Eq. (30)) to obtain the damping matrix. For this example we have

$$\widehat{\mathbf{C}} = 2\mathbf{MT}\left[a_0\mathbf{I} + a_1 \exp\left\{-a_2\left(\mathbf{T} - a_3\mathbf{I}\right)^2\right\} + a_4 \exp\left\{-a_5\left(\mathbf{T} - a_6\mathbf{I}\right)^2\right\}\right] \in \mathbb{R}^{972\times 972}. \tag{50}$$

Again we have compared our damping identification method with the other four methods discussed before. The modal damping factors obtained using the proposed generalized proportional damping matrix in Eq. (50) is shown in figure 16. In the same plot the results obtained from the other methods are also shown. In order to apply the inverse modal transformation method, only the first nine columns of the analytical modal matrix are retained to obtain the truncated modal matrix $\widehat{\mathbf{\Phi}} \in \mathbb{R}^{972\times 9}$. This approach reproduces the damping factors for the first nine modes very accurately. However, beyond the first nine modes the damping factors obtained using the inverse modal transformation method is just zero (that is effectively all the modes become undamped). The best fitted Rayleigh damping matrix for this example is obtained as

$$\widehat{\mathbf{C}}_b = 0.185\mathbf{M} + 1.81 \times 10^{-6}\mathbf{K}. \tag{51}$$

It was not possible to obtain the constants α_j from Eq. (31) using Caughey method because the associated $\mathbf{W}$ matrix became highly ill-conditioned. For the polynomial fit method, only a third-order polynomial could be fitted to avoid the ill-conditioning problem. The best fitted third-order polynomial is case turns out to be

$$\zeta = p_1 + p_2\omega + p_3\omega^2 + p_4\omega^3 \tag{52}$$

where

$$p_1 = 9.61 \times 10^{-4}, \quad p_2 = 1.15 \times 10^{-6}, \quad p_3 = -8.73 \times 10^{-10} \quad \text{and} \quad p_3 = 1.57 \times 10^{-13}. \tag{53}$$

The damping matrix corresponding to the polynomial in Eq. (52) can be obtained as

$$\begin{aligned} \widehat{\mathbf{C}}_d &= 2\mathbf{MT}\left[p_1\mathbf{I} + p_2\mathbf{T} + p_3\mathbf{T}^2 + p_4\mathbf{T}^3\right] \\ &= 2p_2\mathbf{K} + 2(p_1\mathbf{M} + p_3\mathbf{K})\sqrt{\mathbf{M}^{-1}\mathbf{K}} + 2p_4\mathbf{K}\mathbf{M}^{-1}\mathbf{K}. \end{aligned} \tag{54}$$

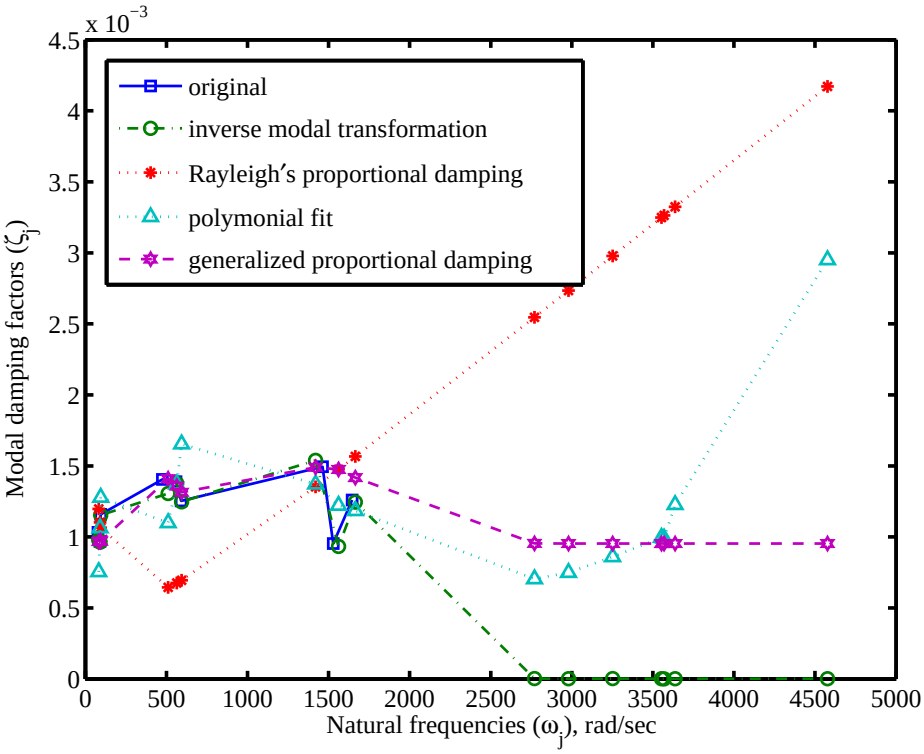

Figure 16: Comparison of modal damping factors using different proportional damping matrix identification method for the clamped plate with slots.

This matrix, like the Rayleigh damping matrix, shows high modal damping values beyond the fitted modes.

CONCLUSIONS

A method for identification of damping matrix using experimental modal analysis has been proposed. The method is based on generalized proportional damping. The generalized proportional damping expresses the damping matrix in terms of smooth continuous functions involving specially arranged mass and stiffness matrices so that the system still posses classical normal modes. This enables one to model variations in the modal damping factors with respect to the frequency in a simplified manner. Once a scalar function is fitted to model such variations, the damping matrix can be identified very easily using the proposed method. This implies that the problem of damping identification is effectively reduced to the problem of a scalar function fitting. The method is simple and requires the measurement of damping factors and natural frequencies only.

The damping matrix identification method was applied to two laboratory based examples involving a free-free beam and a plate with slots. The proposed method was compared to existing methods such as the inverse modal transformation method, Rayleigh's proportional damping Method, Caughey series Method and polynomial fit method. The modal damping factors recalculated using the damping matrix obtained from the proposed generalised viscous damping method agree well with the measured damping factors. The proposed method is applicable to any linear structures provided accurate mass and stiffness matrices are available and the modes are not significantly complex. If a system is heavily damped and modes are highly complex, the proposed identified damping matrix can be a good starting point for more sophisticated analyses.

ACKNOWLEDGEMENTS

SA acknowledges the support of the Engineering and Physical Sciences Research Council (EPSRC) through the award of an advanced research fellowship. SK acknowledges financial support from: Cambridge Commonwealth Trust and Nehru Trust for Cambridge University through the award of Nehru Fellowship; ORS award from CVCP, UK; Bursaries from St. John's college, Cambridge, UK.

APPENDIX I. THE PROOF OF THEOREM 2

Consider the 'if' part first. Suppose $\mathbf{\Phi}$ is the mass normalized modal matrix and $\mathbf{\Omega}$ is the diagonal matrix containing the undamped natural frequencies. By the definitions of these quantities we have

$$\mathbf{\Phi}^T\mathbf{M}\mathbf{\Phi} = \mathbf{I} \tag{55}$$

$$\text{and} \quad \mathbf{\Phi}^T\mathbf{K}\mathbf{\Phi} = \mathbf{\Omega}^2. \tag{56}$$

From these equations one obtains

$$\mathbf{M} = \mathbf{\Phi}^{-T}\mathbf{\Phi}^{-1}, \quad \mathbf{K} = \mathbf{\Phi}^{-T}\mathbf{\Omega}^2\mathbf{\Phi}^{-1} \tag{57}$$

$$\mathbf{M}^{-1}\mathbf{K} = \mathbf{\Phi}\mathbf{\Omega}^2\mathbf{\Phi}^{-1} \quad \text{and} \quad \mathbf{K}^{-1}\mathbf{M} = \mathbf{\Phi}\mathbf{\Omega}^{-2}\mathbf{\Phi}^{-1}. \tag{58}$$

Because the functions $\beta_1(\bullet)$ and $\beta_2(\bullet)$ are assumed to be analytic in the neighborhood of all the eigenvalues of $\mathbf{M}^{-1}\mathbf{K}$ and $\mathbf{K}^{-1}\mathbf{M}$ respectively, they can be expressed in polynomial forms using the Taylor series expansion. Following Bellman (1960) we may obtain

$$\beta_1\left(\mathbf{M}^{-1}\mathbf{K}\right) = \mathbf{\Phi}\,\beta_1\left(\mathbf{\Omega}^2\right)\mathbf{\Phi}^{-1} \tag{59}$$

$$\text{and} \quad \beta_2\left(\mathbf{K}^{-1}\mathbf{M}\right) = \mathbf{\Phi}\,\beta_2\left(\mathbf{\Omega}^{-2}\right)\mathbf{\Phi}^{-1}. \tag{60}$$

A viscously damped system will possess classical normal modes if $\mathbf{\Phi}^T\mathbf{C}\mathbf{\Phi}$ is a diagonal matrix. Considering expression (a) in the theorem and using equations (57) and (58) we have

$$\begin{aligned}\mathbf{\Phi}^T\mathbf{C}\mathbf{\Phi} &= \mathbf{\Phi}^T\left[\mathbf{M}\,\beta_1\left(\mathbf{M}^{-1}\mathbf{K}\right) + \mathbf{K}\,\beta_2\left(\mathbf{K}^{-1}\mathbf{M}\right)\right]\mathbf{\Phi} \\ &= \mathbf{\Phi}^T\left[\mathbf{\Phi}^{-T}\mathbf{\Phi}^{-1}\,\beta_1\left(\mathbf{M}^{-1}\mathbf{K}\right) + \mathbf{\Phi}^{-T}\mathbf{\Omega}^2\mathbf{\Phi}^{-1}\,\beta_2\left(\mathbf{K}^{-1}\mathbf{M}\right)\right]\mathbf{\Phi}.\end{aligned} \tag{61}$$

Utilizing equations (59) and (60) and carrying out the matrix multiplications, equation (61) reduces to

$$\begin{aligned}\mathbf{\Phi}^T\mathbf{C}\mathbf{\Phi} &= \left[\mathbf{\Phi}^{-1}\,\mathbf{\Phi}\,\beta_1\left(\mathbf{\Omega}^2\right)\mathbf{\Phi}^{-1} + \mathbf{\Omega}^2\mathbf{\Phi}^{-1}\,\mathbf{\Phi}\,\beta_2\left(\mathbf{\Omega}^{-2}\right)\mathbf{\Phi}^{-1}\right]\mathbf{\Phi} \\ &= \beta_1\left(\mathbf{\Omega}^2\right) + \mathbf{\Omega}^2\beta_2\left(\mathbf{\Omega}^{-2}\right).\end{aligned} \tag{62}$$

Equation (62) clearly shows that $\mathbf{\Phi}^T\mathbf{C}\mathbf{\Phi}$ is a diagonal matrix.

To prove the the 'only if' part, suppose

$$\mathbf{P} = \mathbf{\Phi}^T\mathbf{C}\mathbf{\Phi} \tag{63}$$

is a general matrix (not necessary diagonal). Then there exist a non-zero matrix $\mathbf{S}$ such that (similarity transform)

$$\mathbf{S}^{-1}\mathbf{P}\mathbf{S} = \boldsymbol{\mathcal{D}} \tag{64}$$

where $\boldsymbol{\mathcal{D}}$ is a diagonal matrix. Using equation (62) and (63) we have

$$\mathbf{S}^{-1}\boldsymbol{\mathcal{D}}_1\mathbf{S} = \boldsymbol{\mathcal{D}} \tag{65}$$

where $\boldsymbol{\mathcal{D}}_1$ is another diagonal matrix. Equation (65) indicates that two diagonal matrices are related by a similarity transformation. This can only happen when they are the same and the transformation matrix is an identity matrix, that is $\mathbf{S} = \mathbf{I}$. Using this in equation (64) proves that $\mathbf{P}$ must be a diagonal matrix.

REFERENCES

Adhikari, S. (2004). "Optimal complex modes and an index of damping non-proportionality." *Mechanical System and Signal Processing*, 18(1), 1–27.

Adhikari, S. and Woodhouse, J. (2001a). "Identification of damping: part 1, viscous damping." *Journal of Sound and Vibration*, 243(1), 43–61.

Adhikari, S. and Woodhouse, J. (2001b). "Identification of damping: part 2, non-viscous damping." *Journal of Sound and Vibration*, 243(1), 63–88.

Balmès, E. (1997). "New results on the identification of normal modes from experimental complex modes." *Mechanical Systems and Signal Processing*, 11(2), 229–243.

Bellman, R. (1960). *Introduction to Matrix Analysis*. McGraw-Hill, Mew York, USA.

Caughey, T. K. (1960). "Classical normal modes in damped linear dynamic systems." *Transactions of ASME, Journal of Applied Mechanics*, 27, 269–271.

Caughey, T. K. and O'Kelly, M. E. J. (1965). "Classical normal modes in damped linear dynamic systems." *Transactions of ASME, Journal of Applied Mechanics*, 32, 583–588.

Chen, S. Y., Ju, M. S., and Tsuei, Y. G. (1996). "Extraction of normal modes for highly coupled incomplete systems with general damping." *Mechanical Systems and Signal Processing*, 10(1), 93–106.

Géradin, M. and Rixen, D. (1997). *Mechanical Vibrations.* John Wiely & Sons, New York, NY, second edition. Translation of: Théorie des Vibrations.

Ibrahim, S. R. (1983). "Computation of normal modes from identified complex modes." *AIAA Journal*, 21(3), 446–451.

Kreyszig, E. (1999). *Advanced engineering mathematics.* John Wiley & Sons, New York, eigth edition.

Newland, D. E. (1989). *Mechanical Vibration Analysis and Computation.* Longman, Harlow and John Wiley, New York.

Phani, A. S. (2004). "Damping identification in linear vibrations," PhD thesis, Cambridge University Engineering Department.

Rayleigh, L. (1877). *Theory of Sound (two volumes).* Dover Publications, New York, 1945 re-issue, second edition.

Ungar, E. E. (2000). "Damping by viscoelastic layers." *Applied Mechanics Reviews, ASME*, 53(6), R33–R38.

Nomenclature

α_1, α_2	proportional damping constants
$\boldsymbol{\alpha}$	a vector containing the constants in Caughey series
$\mathbf{C}$	viscous damping matrix
$\beta_i(\bullet), i = 1, \cdots, 4$	proportional damping functions
$\mathbf{I}$	identity matrix
$\mathbf{K}$	stiffness matrix
$\mathbf{M}$	mass matrix
$\boldsymbol{\Omega}$	diagonal matrix containing the natural frequencies
$\boldsymbol{\Phi}$	undamped modal matrix
$\mathbf{q}(t)$	generalized coordinates
$\mathbf{T}$	a temporary matrix, $\mathbf{T} = \sqrt{\mathbf{M}^{-1}\mathbf{K}}$
$\mathbf{W}$	coefficient matrix associated with the constants in Caughey series
$\boldsymbol{\zeta}$	diagonal matrix containing the modal damping factors
$\boldsymbol{\zeta}_v$	a vector containing the modal damping factors
λ_j	complex eigenvalues, $\lambda_j \approx -\zeta_j\omega_j \pm i\omega_j$
ω_j	natural frequencies
$\widetilde{f}(\bullet)$	fitted modal damping function
ζ_j	modal damping factors
$(\bullet)^T$	matrix transpose
$(\bullet)^{-1}$	matrix inverse
$(\bullet)^{-T}$	matrix inverse transpose
$(\bullet)_{(e)}, (\bullet)^{(e)}$	$(\bullet)$ of e-th element/substructure
$\mathrm{Im}(\bullet)$	imaginary part of $(\bullet)$
$\mathrm{Re}(\bullet)$	real part of $(\bullet)$